ELECTRONIC ABSORPTION SPECTRUM AND π-ELECTRONIC STRUCTURE OF CRYPTOCYANINE

Miloš Titz[a], Antonín Novák[a] and Viktor Řeháк[b]

[a] *Research Institute of Organic Syntheses, 532 18 Pardubice - Rybitví and*
[b] *Institute of Chemical Technology, 532 10 Pardubice*

Received July 14th, 1978

Absorption, fluorescence excitation and APF spectra of cryptocyanine have been measured. Dipole moment of the respective S_1 excited state has been estimated from shifts of the marked maximum of the first absorption band in various solvents. On the basis of quantum-chemical calculations carried out by the PPP method in the approximation of quasi-real geometry we have received the optimum model of π-electronic structure of the cryptocyanine molecule and therefrom the theoretical electronic singlet spectrum inclusive of character of the $S_0 \rightarrow S_1$ transition.

Polymethine dyestuffs represent an important group of dyestuffs used for sensibilization of photographic emulsions; several types are used for dyeing of artificial fibers and in laser technology (pasive Q-switches, active media). Their properties are very interesting from theoretical viewpoints, too, especially so if relationships between structure of the dyestuffs and their spectral properties and photophysical processes are investigated.

Some properties of polymethine dyestuffs including the long-wavelength part of their electronic absorption spectrum were interpreted satisfactorily with the use of free electron model[1]. Calculations on the basis of the HMO model were carried out with special aim to accord with the photosensitizing effect[2], polarographic potentials and energies of the transitions[3]. The PPP method gave good predictions of electronic transitions[4,5], and the methods INDO and CNDO/2 involving also the respective anion (Cl^-, Br^-, I^-) in the calculation showed that nature of the anion affects considerably values of ionization energy and symmetry of MO (ref.[6]).

Any detailed analysis of the calculations carried out for cryptocyanine molecule by the PPP method with the aim of interpretation of its electronic absorption in UV and visible regions has not yet been published.

In connection with research of photochemical properties of cryptocyanine and increase of light stability in the resonator cavity of ruby laser[7] we undertook studies of photophysical processes in its solutions[8,9] and quantum-chemical calculations of its π-electronic structure and electronic absorption spectrum.

EXPERIMENTAL

Cryptocyanine (for photography, Lachema, Brno) was purified by three crystallizations from methanol in absence of light. Its purity was checked by TLC on alumina (Reanal, Brockman II neutral, acetone–methanol 9 : 1) and by the shape of spectrum of its blue and red fluorescence being independent of the exitation wavelength.

The absorption spectra were measured with a Perkin–Elmer 365 spectrophotometer. The fluorescence excitation and APF spectra were measured with a Hitachi–Perkin–Elmer MPF-2A spectrofluorimeter. All the experimental data were recorded on punched tape and processed separately with a computer. The fluorescence excitation spectra were corrected with respect to the inner filter effect and reabsorption as well as with respect to spectral characteristics of the apparatus used. The APF spectra were corrected with respect to the proper polarization of the apparatus.

Description of the Electronic Absorption Spectrum

The electronic absorption spectrum of methanolic solution of cryptocyanine shows several marked, well-separated absorption bands in visible and UV regions (Fig. 1). The very intensive long-wavelength absorption band has two maxima (1·41 and 1·54 μm^{-1}), out of which the less intensive one is shifted to higher energies. In the region 2·30—3·00 μm^{-1} the spectrum is considerably dissected containing five maxima (2·36, 2·51, 2·68, 2·81 and 2·92 μm^{-1}) which are especially observable in the low-temperature excitation spectrum. Fluctuating course of the APF curve in this region indicates several various electronic transitions. Another marked maximum is encountered at 3·22 μm^{-1}. At low temperature two shoulders can be seen in its neighbourhood (3·08 and 3·36 μm^{-1}). Towards higher energies three further absorption bands with gradually increasing intensity were found at room temperature (3·65, 3·97 and 4·54 μm^{-1}). Comparison of the APF curve with the absorption and excitation spectra made it possible to construct the line scheme (Fig. 2A) which was further used for verification of correctness of quantum-chemical calculations.

The cryptocyanine spectrum is characterized by large energy difference between the first absorption band and the second one lying at the beginning of UV region. The difference is at least 0·95 μm^{-1} (1·18 eV) and is probably responsible for some extraordinary properties of the cryptocyanine molecule (the $S_2 \rightarrow S_0$ fluorescence[8], easy saturation of optical transitions, stimulated emission).

Assessment of Dipole Moment in S_1 *State*

The present theory of solvent effect[10] enables a relatively simple determination of the change of dipole moment of a molecule after excitation or calculation of dipole moment of a molecule in any excited state, if the absorption bands belonging to transitions into these states can be well separated from one another. The method is suitable for fluorescence measurements, too. In the linear dependence searched for

$$Y_{ij} = 2(hca_0^3)^{-1}\,\Delta\mu\mu_g X_{ij} + (hca_0^3)^{-1}\,(2D^a + (\Delta\mu)^2) \qquad (1)$$

the slope of the straight line can be used for determination of the value $\Delta\mu = \mu_e - \mu_g$ which is the difference of dipole moments in the excited and the ground states, h is the Planck constant, c is the light velocity in vacuum, a_0 is the Onsager radius of molecular cell which is the same for both the molecule in the ground and the excited

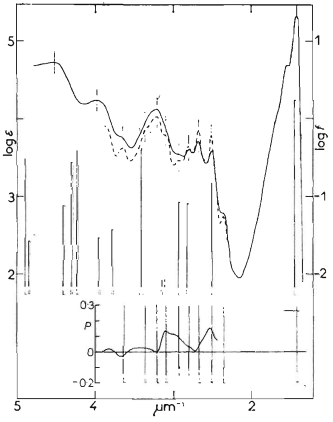

FIG. 1

Absorption Spectrum of Cryptocyanine at Room Temperature (———), Excitation Spectrum at 77 K (– – – –) and APF Spectrum at 77 K

Vertical lines at the top represent energies and intensities of the theoretical singlet transitions, symbols under the lines characterize the polarization of the transitions with respect to y-axis (Table II). The low intensive transitions at 3·15 and 3·12 μm^{-1} could not be represented in the scale of the graph. Vertical lines in the region of APF spectrum correspond to the absorption bands maxima. The symbols under these lines describe the experimentally found polarizations of these bands.

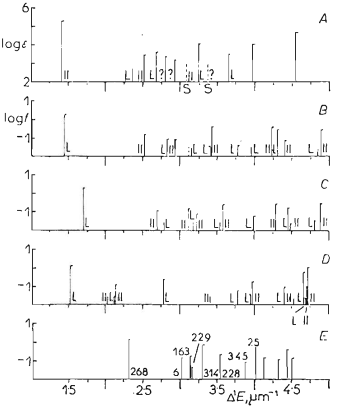

FIG. 2

Experimental A and Theoretical B—E Electronic Absorption Singlet Spectra of Cryptocyanine

The polarization data relate to twofold symmetry axis of the molecule; s shoulder; ? vague polarization; transition denoted by footingless line (———) represents a transition with $\log f < -2$; the transition denoted by dashed line is practically forbidden.

states, and D^a is a parameter depending on energy differences between the final and starting states involved in the transition

$$Y_{ij} = (\nu_j^a - \nu_i^a)/(Q_i - Q_j) \quad \text{and} \quad X_{ij} = (S_i - S_j)/(Q_i - Q_j)\,, \tag{2}$$

where ν_j^a is the wavenumber of the absorption maximum in the j-th solvent. Furthermore

$$Q_i = (n_i^2 - 1)/(2n_i^2 + 1) \quad \text{and} \quad S_i = (E_i - 1)/(2E_i + 1)\,, \tag{3}$$

where n_i and E_i are the refractive index and the dielectric constant of the i-th solvent, respectively. In our case the selection of solvents is considerably limited by solubility of the studied compound (Table I). The experimental data X_{ij} and Y_{ij} processed statistically by the least squares method give the linear dependence

$$Y_{ij} = -2190X_{ij} + 3430 \tag{4}$$

with high correlation coefficient (Fig. 3). The value a_0 for cryptocyanine is not given in literature. This value can be calculated by the Lippert method[11], it is, however, considerably greater (as much as double value) than the obviously more correct data obtained from spectral measurements of structurally similar compounds[12]. If the approximate value $a_0 = 0{\cdot}35$ nm is taken[12] for cryptocyanine, then $\Delta\mu\mu_g = -3{\cdot}133 \,.\, 10^{-58}\ \mathrm{C^2\,m^2}$. Unfortunately the value μ_g is not given in literature, a rough estimate only being possible from data of structurally similar compounds[13] ($1{\cdot}33 \,.\, 10^{-29}$ to $1{\cdot}67 \,.\, 10^{-29}$ Cm). If a mean value $1{\cdot}50 \,.\, 10^{-29}$ Cm is taken, then $\Delta\mu = -0{\cdot}697 \,.\, 10^{-29}$ Cm. From this assessment it follows that the molecule in the first excited singlet state has roughly half dipole moment as compared with the electronic ground state.

This experimental result and the electronic spectrum are considered further experimental basis for verification of selection of theoretical model and the optimization of parameters carried out therein.

THEORETICAL

The calculations of spectral characteristics, dipole moments, π-electron bond orders and π-electron densities were carried out by the standard version PPP of the method LCI SCF ASMO. With respect to the fact that experimental bond lengths and angles of the molecule studied are not known, the mentioned method was predominantly used in the approximation of quasi-real geometry, *i.e.* with variation of the integrals β^c and γ. In an orientation way we also used this method in the approximation of ideal geometry, *i.e.* with constant values β^c and γ, as well as the HMO method. The input data for calculations in the both approximations of the PPP method were

used as it follows: ideal geometry of the cryptocyanine molecule with all bond lengths in the skeleton 0·14 nm and all bond angles 120°.

The bicentric core integrals were calculated according to the formula

$$\beta^{c}_{\mu\nu} = b_{\mu\nu}\beta^{c}_{0} \exp\left(-1{\cdot}862 r_{\mu\nu} + 2{\cdot}597\right). \qquad (5)$$

The bond length between two neighbouring atoms was calculated repeatedly in every iteration according to the Julg formula[14]

$$r_{\mu\nu} = \left(1{\cdot}517 - 0{\cdot}18 p_{\mu\nu}\right)\left(6{\cdot}5/(\vartheta_{\mu} + \vartheta_{\nu})\right)^{1/2}, \qquad (6)$$

TABLE I

Absorption Maxima of Electronic Spectrum of Cryptocyanine in Various Solvents

Solvents	Absorption band, μm^{-1}							
	1		2				3	4
Methanol	1·414	1·530	2·350	2·500	2·675	2·800	3·220	3·960
Acetonitrile[a]	1·410	1·525	2·350	2·500	2·670	2·800	3·220	3·930
Pyridine	1·375	1·500	2·320	2·475	2·640	2·765	3·165	
Tetrahydrofurane	1·382	1·510	[b]				3·320	
Chloroform	1·375	1·505	2·340	2·480	2·660	2·785	3·200	
Ethyl acetate	1·385	1·505	[c]					

[a] The reference solvent; [b] the 2nd band has no marked maximum; [c] very low concentration.

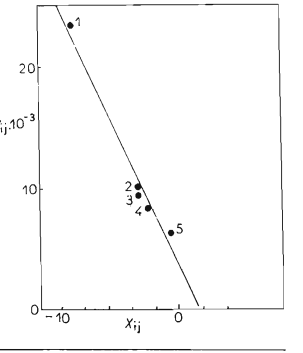

FIG. 3

Dependence of Parameters Y_{ij} and X_{ij} for the First Absorption Band of Electronic Spectrum of Cryptocyanine

1 Ethyl acetate, *2* tetrahydrofurane, *3* chloroform, *4* methanol, *5* pyridine; the reference solvent is acetonitrile.

where $p_{\mu\nu}$ is the π-electron bond order and ϑ_μ and ϑ_ν are the Slater exponents of $2p_z$ atomic orbitals at the atoms μ and ν, respectively. The monocentric repulsion integrals $\gamma_{\mu\mu}$ were obtained by the Parriser approximation[15]

$$\gamma_{\mu\mu} = I_\mu - A_\mu , \qquad (7)$$

where I_μ and A_μ are the ionization potential and the electron affinity of the atom μ in the given valence state and surroundings, respectively. The bicentric repulsion integrals $\gamma_{\mu\nu}$ ($\mu \neq \nu$) were calculated according to the Mataga and Nishimoto approximation[16].

The mesomeric structures given in Scheme 1 indicate a relatively complex π-electronic structure of the molecule studied. The structure *III* localizes positive charge of the cation at one centre, *viz.* central carbon atom of the odd connecting chain considering, furthermore, the both nitrogen atoms as pyrrole-like nitrogens but in six-membered ring. The mutually complementar structures *I* and *II*, however, denote the both nitrogen atoms as the competing site of positive charge, indicating also that the nitrogen atoms cannot be considered strictly pyrrole-like in six-membered ring, as they are in the structure *III*.

Fig. 2*A* gives schematically the electronic absorption spectrum of cryptocyanine (see Experimental – Description of Spectrum), Figs 2*B*–*E* represent theoretical electronic spectra for three various models of the studied molecule (*C*–*E*). These theoretical spectra were obtained by the PPP method in approximation of quasi-real geometry with the standard parameters given below. The result given in the part *B* represents the theoretical spectrum obtained by a parameter study (see below) within the model C which agrees best with experimental spectrum.

The following parameters were used in the calculations the results of which are given in Figs 2*B*–*E*:

Atomic core X	*I*, eV	*A*, eV	*Z*	ϑ	b_{C-X}	model	
C^+	11·42	0·58	1	3·25	1·0	B–E	
N^{2+} (pyrrole resp. amine	27·30	9·30	2	2·67	0·8	C(B)	}
type)	(15·0)						*E*
N^+ (pyridine type)	14·10	1·80	1	3·90	1·0	D	}

the value β_0^c in Eq. (5) is −2·318 eV; the *I* date of the N^{2+} atomic core (in brackets) was obtained by the parameter study (see the theoretical spectrum in Fig. 2*B*). The configuration interaction in the base of the monoexcited configuration functions is limited to five highest occupied and five lowest virtual SCF molecular orbitals from which these configuration functions are formed by monoexcitation of electron.

Parameter study. In all quantum-chemical calculations, be it by HMO or PPP method, the cryptocyanine molecule was considered without ethyl groups and without

any simulation of the anion effect. The first orientation calculations by the PPP method were carried out with standard parameters for carbon atom and nitrogen atom of pyrrole type (see Theoretical) either in approximation of ideal geometry (constant β^c and γ values) or in that of quasi-real geometry (varying β^c and γ values). The theoretical spectra obtained by calculations with these approximations were considerably hypsochromically shifted as compared with experiment (Figs 2*A* and 2*C*), the results obtained in approximation of ideal geometry being less suitable. However, not regarding the considerable hypsochromic shift of these theoretical spectra, it can be stated that the both approximations reflect the substantial features of the experimental absorption spectrum. This relative success together with unwanted hypsochromic shift of the whole spectrum made us to propose several models of the studied molecule and carry out their parameter studies within both the PPP and HMO methods.

Four characteristic features of long-wavelength part of the experimental absorption electronic spectrum of the cryptocyanine molecule were selected to criticize the results obtained by the parameter studies of the models *C*, *D*, and *E*, *viz.* *1*) the considerably intensive first absorption band in the long-wavelength spectral region ($\tilde{\nu}_{max} = 1{\cdot}41\ \mu m^{-1}$) which was previously[8] proved to be formed by only one electronic transition; *2*) the broad region between the first and the second absorption band having the magnitude of minimum $0{\cdot}93\ \mu m^{-1}$; *3*) the absorption bands belonging to the absorption region $2{\cdot}34$ to $2{\cdot}94\ \mu m^{-1}$ are relatively less intensive, especially so if compared with the first absorption band; *4*) relative polarization of the absorption bands in the absorption region $2{\cdot}34$ to $2{\cdot}94\ \mu m^{-1}$ with respect to polarization of the first absorption band (Table II, Fig. 1).

The model C(B) is identical with the mesomeric structure *III* (Scheme 1), the model

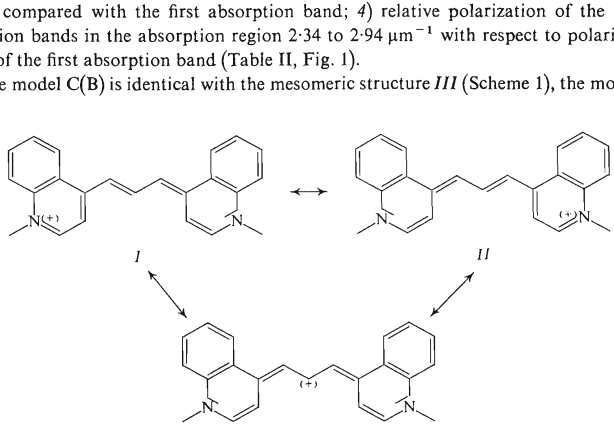

I *II* *III*

SCHEME 1

TABLE II

Theoretical Singlet Transitions $S_0 \rightarrow S_n$ and Theoretical Spectral Characteristics Thereof[a]

$S_0 \rightarrow S_n$ μm^{-1}	Sym. state	log f	M_x	M_y	$\sphericalangle(\boldsymbol{M}, y)$	Main conf.	Next significant conf.	$\lvert\mu\rvert$ 10^{29} Cm $\sphericalangle(\mu, C_2)$
1·447	$^1B_2$	0·24	0·000	3·314	∥	1,1′ (96·6)		1·201 ∥
2·516	$^1A_1$	—0·83	0·736	0·000	⊥	2,1′ (92·8)		1·002
2·823	$^1B_2$	—1·09	0·000	—0·517	∥	3,1′ (89·1)		0·310 ∥
2·932	$^1A_1$	—1·07	—0·515	0·000	⊥	1,2′ (95·1)		1·508 ∥
3·119	$^1A_1$	—4·53	—	—	—	4,1′ (42·3)	1,4′ (31·5)	
3·146	$^1B_2$	—2·33	0·000	0·117	∥	1,3′ (40·6)	5·1′ (30·5)	
3·402	$^1B_2$	—1·56	0·000	—0·274	∥	5,1′ (55·0)	1,3′ (33·7)	
3·409	$^1A_1$	—0·38	1·059	0·000	⊥	1,4′ (43·7)	4,1′ (43·0)	
3·783	$^1B_2$	—1·42	0·000	—0·305	∥	1,5′ (77·2)	2,2′ (10·9)	
3·955	$^1B_2$	—1·53	0·000	0·264	∥	2,2′ (75·9)	1,5′ (15·5)	
4·228	$^1A_1$	—0·41	—0·925	0·000	⊥	2,3′ (29·6)	3,4′ (22·1); 3,2′ (20·7)	
4·302	$^1B_2$	—0·56	0·000	0·749	∥	2,4′ (38·0)	3,3′ (24·9)	
4·406	$^1A_1$	—1·12	0·400	0·000	⊥	3,2′ (80·0)		
4·844	$^1B_2$	—1·57	0·000	0·226	∥	4,2′ (88·0)		
4·888	$^1A_1$	—0·52	—0·752	0·000	⊥	5,2′ (87·0)		
5·010	$^1A_1$	—0·63	—0·524	0·000	⊥	2,5′ (70·1)		

[a] The x-axis is identical with the C_2 symmetry axis of the molecule, the z-axis is perpendicular to the plane of the molecule; M_x and M_y are the x and y components of the transition dipole moment vector, respectively; $\sphericalangle(\boldsymbol{M}, y)$ is the angle between the transition dipole moment vector and y-axis; $|\mu|$ is the magnitude of the dipole moment vector in Cm; $\sphericalangle(\mu, C_2)$ is the angle between the dipole moment vector and $C_2(x)$ symmetry axis.

E corresponds to the structure *I* or *II*, and the model D corresponds to the structure having the both nitrogen atoms of pyridine type; the model D has 22 π-electrons, *i.e.* 2π-electrons less than the models C(B) and E.

Out of the parameter studies as well as the calculations carried out for standard parameters of the C, D and E models of cryptocyanine molecule, the model C proved to be the most acceptable having considerably lowered ionization potential of its pyrrole-like nitrogen atoms (Fig. 2*B*). This lowering of the ionization potential value from 27·30 eV to 15·0 eV with retained standard value of electron affinity 9·30 eV reflects best the π-electronic structure of the studied molecule represented by the mesomeric structures *I* and *II*. It is perhaps noteworthy to mention the same course of dependences $E(N \rightarrow V_1)$ of the transition on the value α^{eff} for the nitrogen atoms which were obtained by the HMO method within the C and D models and the energies of the first singlet transition obtained by the PPP method in dependence on ionization potential of the nitrogen atoms in the same models (Fig. 4). The correlation diagram of the frontier SCF molecular orbitals obtained by the calculation

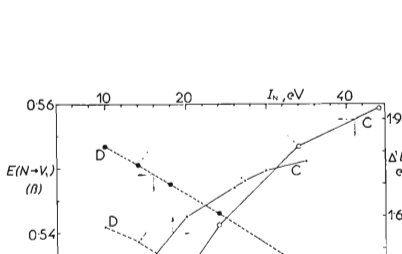

FIG. 4

Dependence of $E(N \rightarrow V_1)$ and $\Delta^1 E_1$ in the Models C and D of Cryptocyanine Molecule on Values α_N^{eff} and I_N, respectively

The arrows denote the values $\Delta^1 E_1$ and $E(N \rightarrow V_1)$ for standard parameters; the HMO parameters: $\delta_{-\bar{N}=} = 0{\cdot}5\beta$, $k_{C-N} = 1{\cdot}0\beta$, $Z^{\pi}_{-\bar{N}=} = 1$ for the pyridine-like nitrogen atom of the model D and $\delta_{-NH-} = 1{\cdot}5\beta$, $k_{C-NH-} = 0{\cdot}8\beta$, $Z^{\pi}_{-NH-} = 2$ for the pyrrole-like nitrogen atom of the model C — these parameters are constants in the characteristic relations: $\alpha_X^{eff} = \alpha_C^{eff} + \delta_X \beta_{C-C}^{eff}$ and $\beta_{C-X}^{eff} = k_{C-X}\beta_{C-C}^{eff}$; ○, ● represent the HMO calculations; +, × denote the PPP calculations; the point B in the dependence C (PPP) denotes the result of the optimum version of calculation of the model C.

versions B to E is given in Fig. 5, the double-headed arrow denoting the HOMO-LUMO interval and the dashed line denoting the mutual relation of the highest occupied and the lowest virtual orbitals. The not very dramatic changes (no level crossing) between the calculation versions B and C stand in contrast with the marked shifts of SCF levels in the models D and E, which also corresponds to their different theoretical spectra in Fig. 2. The unsubstantial changes in the correlation graph between the calculation versions B and C agree with similar minor changes in the values of the π-electron bond orders and π-electron densities, the only exception being the π-electron density decrease at nitrogen atom (by 0·1) in the version B. Quite contrary is the situation of the models D and E where considerable crossing of values of bond orders and electron densities is encountered for the individual bonds and centres; thus it can be stated the π-electronic structure of the models D and E differs considerably from that of the model C in both versions of calculation. In spite of this differences in π-electronic structure let us mention some important common features of the theoretical spectra which can be seen in Fig. 2: in all the three models the first $^1(\pi\pi^*)$ transition is considerably intensive and means always a transition to the state with predominant mono-excited configuration 1,1′ which is polarized perpendicularly to twofold axis; between the first and the second transition there is a variable, nevertheless a rather large region of forbidden energies; the second and several further transitions are markedly less intensive than the first one. However, all the three considered models have the same topology, which could possibly explain the above-mentioned common features of the theoretical spectrum, whereas effects of parameters of heteroatoms and number of π-electrons represent an effect of higher order which makes itself felt mainly in the shift of transitions in these spectra.

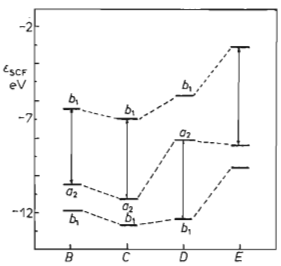

FIG. 5

Correlation Diagram of Frontier SCF MO's for the Models C to E and for the B Version of Calculation within the Model C

RESULTS AND DISCUSSION

In the above paragraph we gave the results of parameter studies within the models C, D, E, the version of calculation B within the model C having proved the optimum for expressing the experimental absorption electronic spectrum by the theoretical one (Fig. 2). Table II gives the numerical results obtained by the PPP method concerning the first $S_0 \rightarrow S_n$ transitions. The first four singlet excited states are very "pure" states with fairly high weight coefficients for the respective predominant monoexcited configurations; there follows a series of singlet excited states where two dominant monoexcited configurations have comparable weight coefficients, transitions to "pure" excited singlet states again corresponding to short wavelength part of spectrum. Table III gives the first five excited triplet states which are (except for the first one) less "pure" than the corresponding singlet states.

Fig. 6 represents π-electronic structure of the cryptocyanine molecule in the ground state (*6a*) and the first four excited singlet states (*6b – e*); the circles represent charges at the individual centres, the measure of the double-bond character of the bonds in the studied cation being also indicated. In all the given cases the both nitrogen atoms represent the dominant site of positive charge (in accord with the structures *I* and *II* in Scheme 1); the central atom of the odd chain carries positive charge only in the ground and the fourth excited states (structure *III*). Charge alternation is only encountered in some parts of the molecule, the most marked one being in the ground state. Values of π-electron bond orders do not show such a variability, which is not surprising as the molecule is fairly rigid; some more striking changes are observed with the fourth excited state in which the outer bond of the carbon chain (B) has the least double-bond (aromatic) character, whereas the bond K becomes aro-

TABLE III
Theoretical[a] Triplet States T_n

$T_n \equiv S_0 \rightarrow T_n$ μm^{-1}	Sym. state	Main conf.	Next significant conf.	$\lvert\vec{\mu}\rvert$ 10^{29} Cm	$\sphericalangle(\mu, C_2)$
0·707	$^3B_2$	1,1′ (97·6)		1·211	
1·660	$^3A_1$	1,2′ (53·1)	2,1′ (45·4)	1·478	
2·113	$^3A_1$	2,1′ (46·1)	1,2′ (39·2); 3,2′ (11·4)	1·099	
2·300	$^3B_2$	3,1′ (79·5)	2,2′ (16·3)	0·266	
2·660	$^3A_1$	4,1′ (49·8)	1,4′ (23·5)	0·617	

[a] The *x*-axis is identical with the C_2 symmetry axis of the molecule; $\lvert\vec{\mu}\rvert$ is the magnitude of dipole moment vector in Cm; $\sphericalangle(\mu, C_2)$ is the angle between the dipole moment vector and $C_2(x)$ symmetry axis.

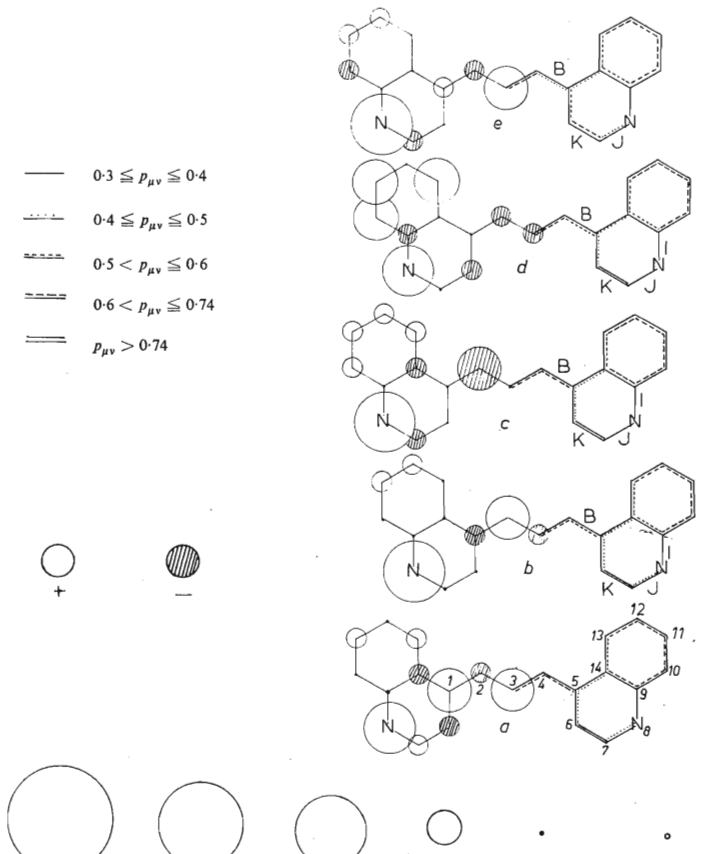

FIG. 6

π-Electronic Structure of Cryptocyanine Molecule in the Ground (*a*) and the First Four Excited Singlet States (*b* — *e*) in the B Version of Calculation of Model C

matic loosing some of its hitherto double-bond character. The bond I with the greatest single-bond character retains its clean-cut nature, whereas character of the second bond (J) of the nitrogen atom is somewhat more variable. Characteristic feature of the molecule in all the five cases is its considerably aromatic six-membered nucleus in which there is no heteroatom and which is not bound with the odd carbon chain. On the basis of this differentiation between "double", "single" and aromatic bonds we tried to find the character of the first singlet $\pi\pi^*$ transition; according to occurrence of bonds with strongly decreased double-bond character (partial interruption of conjugation) we divided the cryptocyanine molecule into five-membered connecting chain (1 – 5), two ethylenic bonds K (6 – 7), two nitrogen atoms (8) and two not much perturbed benzene nuclei (atoms 9 – 14). By comparison of π-electron densities at individual atoms of the subsystems thus formed in the ground and the first excited singlet states we obtained the character of the transition $S_0 \rightarrow S_1$ which is formed mainly (4/5) by local transitions and to minor degree (1/5) by charge-transfer transitions (Table IV)[17]. The found character of the $S_0 \rightarrow S_1$ transition agrees with the not very large change of theoretical π-electronic dipole moment which has the values $1{\cdot}484 \cdot 10^{-29}$ Cm and $1{\cdot}201 \cdot 10^{-29}$ Cm in the ground and the first excited singlet states, respectively, which agrees very well with experimental values ($1{\cdot}50 \cdot 10^{-29}$ Cm and $0{\cdot}803 \cdot 10^{-29}$ Cm), the direction of vector of the dipole moment lying, of course, in the C_2 axis of the molecule. Dipole moments of further singlet and triplet excited states are given in Tables II and III, respectively.

TABLE IV
Character of $S_0 \rightarrow S_1$ Transition[a]

Δq^s	$\Delta q^{CT(D-A)}$	(%)	$\Delta q^{LT(A)}$	(%)	$\Delta q^{LT(D)}$	(%)
0·667	0·089 	(14) chain (1—5)	0·330 chain (1—5)	(49)	—	—
	0·032 	(5) ethylene (6, 7)	0·114 ethylene (6,7)	(17)	—	—
	0·014 	(2) benzene (9—14)	0·088 benzene (9—14)	(13)	—	—

[a] For numbering of atoms see Fig. 6; Δq^s total change of charge in the studied transition; Δq^{CT} charge transfer from the subsystem D to A in the given transition; Δq^{LT} change of the charge in the subsystem A or D in the given transition.

REFERENCES

1. Kuhn M.: Helv. Chim. Acta *31*, 1441 (1948).
2. Brooker L. G. S. in the book: *The Theory of Photographic Process* (T. H. James, Ed.), Chap. 11. McMillan, New York 1966.
3. Sturmer D. M., Gaugh W. S.: Photogr. Sci. Eng. *17*, 146 (1973).
4. Leupold D.: Z. Phys. Chem. (Leipzig) *223*, 405 (1963).
5. Leubner I., Dehler J., Hohlneicher G.: Ber. Deut. Chem. Ges. *71*, 560 (1967).
6. Weinstein H., Apfelderfer B., Berg R. A.: Photochem. Photobiol. *18*, 175 (1973).
7. Řehák V., Poskočil J.: This Journal *41*, 1005 (1976).
8. Řehák V., Novák A., Titz M.: Chem. Phys. Lett. *52*, 39 (1977).
9. Řehák V., Titz M., Novák A.: This Journal, in press.
10. Varma C. A. G. O., Groenen E. J. J.: Rec. Trav. Chim. Pays-Bas. *91*, 296 (1972).
11. Lippert E.: Z. Electrochem. *61*, 962 (1957).
12. Wert W., Geddes A. L.: J. Phys. Chem. *68*, 837 (1964).
13. Brooker L. G. S., White F. L., Keyes G. H., Smyth C. P., Oesper P. F.: J. Amer. Chem. Soc. *63*, 3192 (1941).
14. Julg A.: J. Chim. Phys. Physicochim. Biol. *55*, 413 (1958); *57*, 19 (1960).
15. Pariser R.: J. Chem. Phys. *21*, 568 (1953).
16. Nishimoto K., Mataga N.: Z. Phys. Chem. (Frankfurt) *12*, 335 (1957); *13*, 140 (1957).
17. Nepraš M., Titz M.: Int. J. Quantum Chem. *16*, 543 (1979).

Translated by J. Panchartek.